Title	Role of Surface Tension in Fusion Welding (Part 2) : Hydrostatic Effect
Author(s)	Matsunawa, Akira; Ohji, Takayoshi
Citation	Transactions of JWRI. 1983, 12(1), p. 123-130
Version Type	VoR
URL	https://doi.org/10.18910/9406
rights	
Note	

Role of Surface Tension in Fusion Welding (Part 2)†
— Hydrostatic Effect —

Akira MATSUNAWA* and Takayoshi OHJI**

Abstract

The paper describes the mathematical methods of calculating the surface profiles of hunging liquid supported by capillary action in gravitational field and their application to determine the allowable size parameters for self-suspension of molten pool in full penetration welding and of molten droplet formed at the electrode tip. It is also briefly described the fluidmechanical instabilities of liquid membrane and cylinder.

KEY WORDS: (Capillarity), (Surface Tension), (Surface Profile), (Pendant Drops), (Fusion Welding), (Metal Transfer)

1. Introduction

In the part 1 of this series article[1] were described an analytical solution of the surface profiles of two-dimensional liquid bed placed on a flat plate or at the corner of two plates intersected, and also their applicability to actual weld beads. Other particular interests relating to the static effects of surface tension in fusion welding may be the self-supporting of the molten pool of full penetration welding of thin plate or overhead position welding, and the phenomena of liquid pendant drop formed at the tip of electrode or filler wire. To the former, a two-dimensional analysis is expected to be still effective, while, to the latter, the three-dimensional treatment is essentially necessary. The aims of this report is, therefore, to review the theoretical approaches on supporting liquid drops only by capillary pressure in the gravitational field. Though there have been many theoretical or analogous methods available on the subjects, the authors have mainly referred to the works conducted by Bashforth and Adams[2], and Nishiguch and Ohji[3].

2. Two-dimensional Analysis of Suspended Liquid by Capillary Pressure

2.1 Static pressure balance and allowable width of liquid for self-support

Catastrophic collapse of molten pool, so called burn-through, is a significant problem in full penetration welding of root bead formation in flat position, and one has to carefully control the bead parameters for a given plate thickness or to employ some mechanical backing system. Not only in the flat position, the situation is the same in the overhead or any other positions. If no artificial backing equipment such as mechanical or electromagnetic method is employed, the capillary action is the only possible mechanism to support the molten pool steadily. However, there was no systematic research found on this matter for a long time. In 1978, one of the authors (T.O.) attempted to establish a criterion on this matter by his previously settled mathematical modelling[3]. Here will be reviewed the results in case of full penetration welding of horizontal plate.

Let us consider a two-dimensional molten pool of full penetration welding as shown in **Fig. 1**. For the sake of simplicity, the top surface is assumed to be flat. The basic equation of pressure balance at the point P on liquid surface are the same with those described in the previous paper[1], i.e.,

$$\frac{\sigma}{R_0} - \rho g y = \frac{\sigma}{R} \tag{1}$$

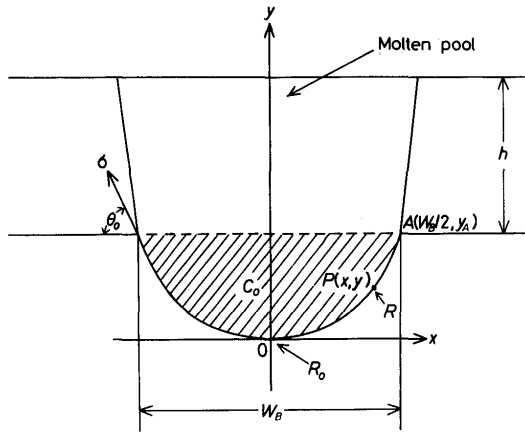$$\frac{1}{R} = \frac{(d^2 y/dx^2)}{\{1 + (dy/dx)^2\}^{3/2}} \tag{2}$$

Fig. 1   Two-dimensional model of molten pool in full penetration welding[3]

From the above relations,

$$\frac{1}{\{1+(dy/dx)^2\}^{1/2}} = \frac{\rho g}{2\sigma}y^2 - \frac{1}{R_0}y + 1 \equiv P(y) \qquad (3)$$

Therefore, the surface profile of backside pool is expressed by elliptical integral as

$$x = \pm \int_0^y \frac{P(y)}{\sqrt{1-P^2(y)}} \, dy \qquad (4)$$

Supposing θ_0 the contact angle between the liquid and soled plate, the width of root bead is

$$w_B = 2 \int_0^{y_a} \frac{P(y)}{\sqrt{1-P^2(y)}} \, dy \qquad (5),$$

and hence y_a is readily obtained from the eq. (3) putting $dx/dy = \tan \theta_0$ at $y = y_a$.

$$y_a = \frac{1}{2R_0}\frac{2\sigma}{\rho g} - \sqrt{\frac{2\sigma}{\rho g}}\sqrt{\frac{1}{4R_0^2}\frac{2\sigma}{\rho g} - (1-\cos\theta_0)} \qquad (6)$$

Considering the force balance per unit length along pool lengh, the cross sectional area C_0 of hatched region in Fig. 1 can be obtained as

$$\rho g(C_0 + w_B h) = 2\sigma \sin\theta_0$$

$$\therefore \ C_0 = \frac{2\sigma}{\rho g}\sin\theta_0 - w_B h \qquad (7)$$

where, h is the plate thickness.
Here, a flat top surface is supposed, and then the pressure balance at the origin of coordinate is

$$\frac{\sigma}{R_0} = \rho g(y_a + h) \qquad (8)$$

Substituting eq. (6) into eq. (8), one obtains

$$h = \sqrt{\frac{2\sigma}{\rho g}}\sqrt{\frac{\sigma}{2\rho g R_0^2} - (1-\cos\theta_0)} \qquad (9)$$

As derived in the above, one can calculate the critical self-supporting condition of liquid from eqs. (5), (7) and (9) in the terms of bead width, plate thickness and cross section of the root bead reinforcement.
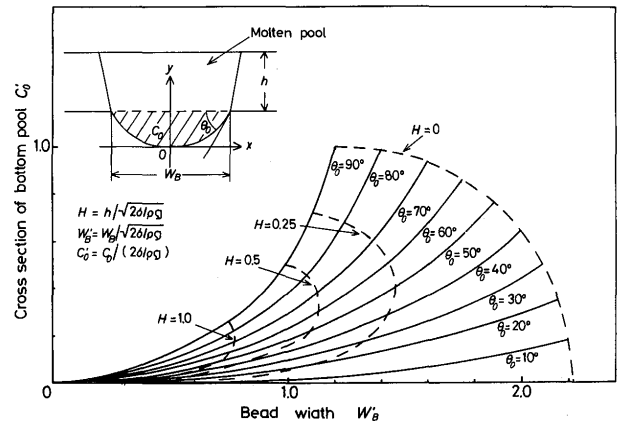

Fig. 2   Effect of bead width and liquid volume on surface profile of self-suspended bottom pool[3]

Figure 2 shows the calculated results of allowable conditions to support molten pool by capillary pressure for various plate thickness. Here, all parameters relating to distance and area are expressed in non-dimensional form as

$$W_B = w_B/\sqrt{2\sigma/\rho g}$$

$$H = h/\sqrt{2\sigma/\rho g}$$

$$C_0 = c_0/(2\sigma/\rho g).$$

In the figure, the solid lines show the W_B-C_0 curve under the constant contact angle, while the broken lines for the constant plate thickness. For a given plate thickness, the allowable width of back side pool changes with the contact angle. In case of $H = 0.25$, for example, the maximum allowable width is obtained at the angle around $50°$ and its value is 1.43 times of the capillary constant. In the width range just below the maximum value, there are two possible contact angles at a certain width.

The maximum allowable width decreases with the increase in plate thickness and it tends to occur at the angle near $90°$ for the thickness over $H = 1.0$. In such situation, one can reasonably assume that the surface profile of liquid becomes semi-circular shape due to small value of w_B compared with the capillary constant. Name-

ly, $R_0 \approx w_B/2$, $\theta_0 = 90°$, and $w_B \ll (2\sigma/\rho g)$ Therefore, the eq. (9) becomes

$$h = \sqrt{\frac{2\sigma}{\rho g}} \sqrt{\frac{2\sigma}{\rho g w_B^2} - 1}$$

$$\approx \sqrt{\frac{2\sigma}{\rho g}} \sqrt{\frac{2\sigma}{\rho g w_B^2}}$$

and the maximum allowable width is approximated as
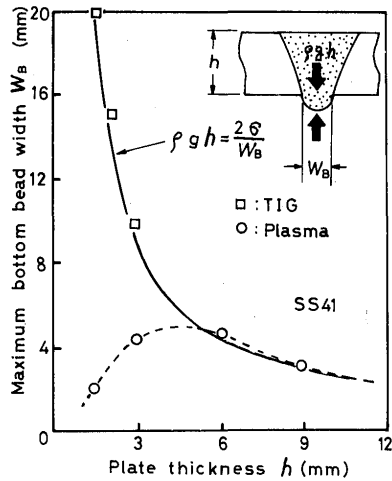
$$w_B \approx \frac{2\sigma}{\rho g h} \tag{10}.$$

Fig. 3   Relation between plate thickness and allowable root bead width for self-support[4]

As seen in **Fig. 3**, the relation (10) well fits to the actual data of low current TIG arc, where arc pressure is very low. While, in a key-hole process by plasma arc, the relation does not hold in thinner plates than 5 mm in thickness. The primary reason of extremely small value of allowable width in plasma arc process has been discussed from the view points of bridging phenomena of two liquid drops at the rear part of key hole.[4]

The above were the cases that the liquid has a flat surface at the top. If the top surface is dented, the maximum allowable width of root bead for self-support becomes wider for the same plate thickness as shown in **Fig. 4**. However, the surface dented beads are generally not desirable from the practical view point.

The maximum allowable width of root bead for self-support of molten pool decreases inverse proportionally with the increase in plate thickness. In case of steel, for instance, the width becomes only about 2 mm in order to support the pool of 10 - 12 mm thick plate, which is practically very hard to steadily maintain such a narrow root bead by the conventional arc processes
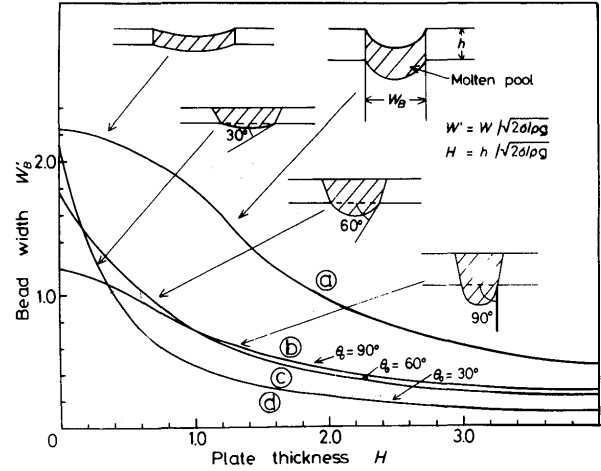

Fig. 4   Effect of surface profile of top-side pool on allowable root bead width for self-support of molten pool[3]

except EB or Laser welding. It is, therefore, necessary to employ some supporting method, i.e., backing system, for the one side - single pass welding of heavy section plate.

There are several types of backing system available, i.e., (1) solid backing, (2) flux backing, (3) gas backing, and (4) their combination. But, even if a backing system is adopted, one often experiences unstable root bead formation when the width of back-side bead is too wide. The phenomena are supposed to be associated by some kind of fluidmechanical instability.

2.2 Rayleigh-Taylor instability of liquid membrane

In order to examine the stability of molten pool, Ohji[3] conducted an experiment to obtain an arc melted liquid disc by gas backing process as shown in **Fig. 5**, where the surface profile of backside pool can be controlled by regulating the gas pressure.
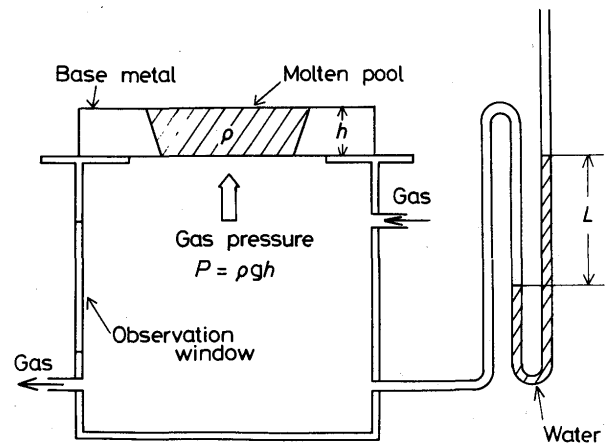
Let d be the diameter of a circular liquid disk or
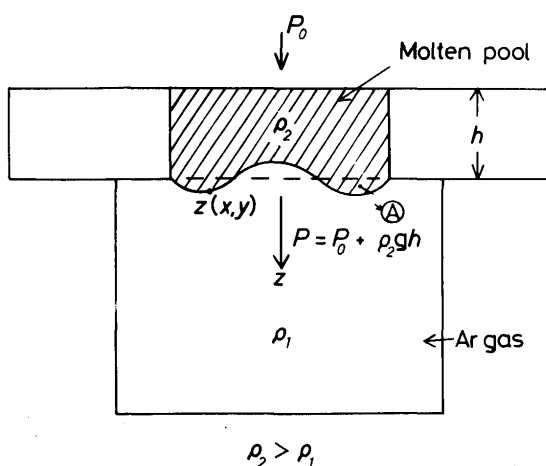

Fig. 5   Gas backing system[3]

Fig. 6   Occurrence of Rayleigh-Taylor instability in large size molten pool[3]

membrane, then there could be no critical value of d for static equilibrium if the surface were kept perfectly flat by gas pressure. Now let us suppose a slight displacement of surface from its equilibrium as illustrated in **Fig. 6**, then the gravity head of pool at the position A becomes higher than the gas pressure. If the wavelength of displacement is small enough, the capillary pressure associated by a curved surface acts to recover the surface back to equilibrium state and hence the pool is stable. While, if the wavelength is large, no recovering effect is expected and the liquid membrane collapses from the A part and pool is unstable. Such unstable phenomenon that occurs when a heavier fluid is supported by a lighter in opposition to the gravity is called Rayleigh-Taylor Instability. As the characteristic wavelength is longer in larger membrane, the Rayleigh-Taylor instability is likely to occur in large pools. The capillary pressure affects to restrict the instability, and then the higher the capillary constant the larger the critical size becomes.

Table 1   Maximum diameter of liquid membrance that can be supported in gas backing process

Backing Gas	Plate Thickness (Mild Steel)			
	$h = 2.3$ mm	$h = 3.2$ mm	$h = 4.5$ mm	$h = 6.0$ mm
CO_2	22 mm	21 mm	22 mm	22 mm
Ar	27 mm	28 mm	28 mm	28 mm

Table 1 shows the measured maximum diameter of liquid steel membrane before the instability took place in gas backing experiment. It is obvious that the critical diameter of stable membrane is larger in Argon atmosphere where the surface tension is higher than in oxidizing gas (refer to Part 1), and there found no significant differences in plate thickness. In case of the welding of root bead in flat position, Ohji concluded after the calculation and experiments that the Rayleigh-Taylor

instability becomes significant when the root bead width is more than 2.2 times of the capillary constant.

3. Pendant Drops of Liquid (Three-dimensional Analysis)

3.1 Calculated profile of hunging drop

We have so far described the two-dimensional analyses of static capillary actions in relation to weld pool phenomena. In real weld puddle, the shape is not two-dimensional and there exists complicated flow, and thus the previous modelling has of course limitation of applicability. However, the two-dimensional analyses have successfully brought one the clear sight of the welding phenomena. In this sense, a mathematical analysis of the three-dimensional liquid profile in general case would be desirable, if it would be possible. Only the case of axisymmetrical liquid droplet has been well analysed. In relation to metal transfer of electrode or filler wire in welding, the shape analysis of pendant drop has been an important subject. In 1883, Bashforth and Adams[2] published an excellent book in which they described the mathematical methods of solving the precise profile of axisymmetric liquid drops in gravitational field. In the following will be reviewed their method in case of a hunging drop.

Suppose revolution of surface formed by uniform surface tension at the boundary of liquid as described in **Fig. 7**. Let z be the axis of revolution measured upward and the point where it meets the free surface be the origin. If R_1 and R_2 are the principal radii of curvature at any point P(x, z) of the liquid surface, the capillary pressure is
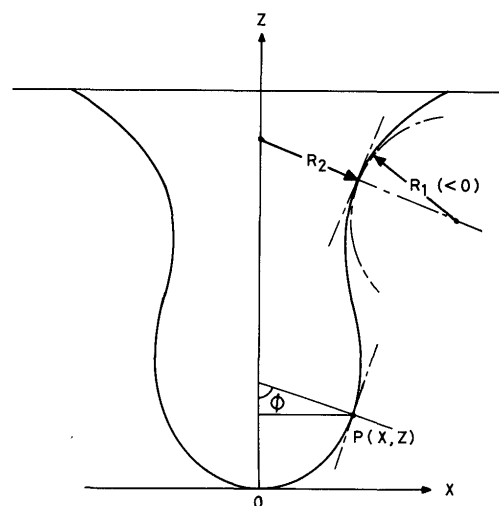

Fig. 7   Pendant drop of liquid and related parameters

$$p = \sigma \left(\frac{1}{R_1} + \frac{1}{R_2} \right) \qquad (11),$$

and the gravity head of liquid at the same height with point P is

$$p = -\rho g z + C \qquad (12),$$

where, C is constant.
The equilibrium condition is then

$$\frac{1}{R_1} + \frac{1}{R_2} = \frac{1}{\sigma}(C - \rho g z) \qquad (13).$$

If R_1 and R_2 are the radii of curvature in the profile plane (medional plane) and that of the inscribed disc plane respectively, they can be expressed as

$$\frac{1}{R_1} = \frac{d^2 z/dx^2}{\{1 + (dz/dx)^2\}^{3/2}} \qquad (14)$$

$$\frac{1}{R_2} = \frac{sin\phi}{x}$$

$$= \frac{dz/dx}{x\{1 + (dz/dx)^2\}^{1/2}} \qquad (15),$$

where ϕ is the angle that the normal to the surface at point P makes with the axis of revolution. (Fig. 7)
Let R_0 be the radius of curvature at the origin, then

$$R_1 = R_0 \text{ and } \lim_{x \to 0} (x/sin\phi) = R_0 \text{ at } z = 0.$$

Hence, the constant C in eq. (13) becomes

$$C = \frac{2\sigma}{R_0} \qquad (16).$$

Introducing non-dimensional parameters as

$$\beta = \frac{\rho g R_0^2}{\sigma}$$

$$\Lambda = R_1/R_0$$

$$\xi = x/R_0$$

$$\zeta = z/R_0,$$

the eq. (13) becomes

$$\frac{1}{\Lambda} + \frac{sin\phi}{\xi} = 2 - \beta\zeta \qquad (17),$$

or its equivalent differential equation of 2nd order as

$$\frac{d^2\zeta}{d\xi^2} + \{1 + (\frac{d\zeta}{d\xi})^2\}\frac{1}{\xi}\frac{d\zeta}{d\xi} = (2-\beta\zeta)\{1 + (\frac{d\zeta}{d\xi})^2\}^{3/2}$$

$$(18).$$

The two arbitrary constants which appear in the integral of eq. (18) must be determined by the condition that

$$\zeta = 0 \text{ and } d\zeta/(\xi d\xi) = 1 \text{ when } \xi = 0.$$

As it is not able to find the general relation between ξ and ζ in the eq. (18), one must solve it by numerical or graphical methods. In general, the objective curve is determined in series proceeding according to ascending powers of the increment of the chosen independent variable. Namely, one can determine a small portion of the curve starting from a known point, and one starts again from the end of this portion for determining another small portion. Repeating this procedure, one can
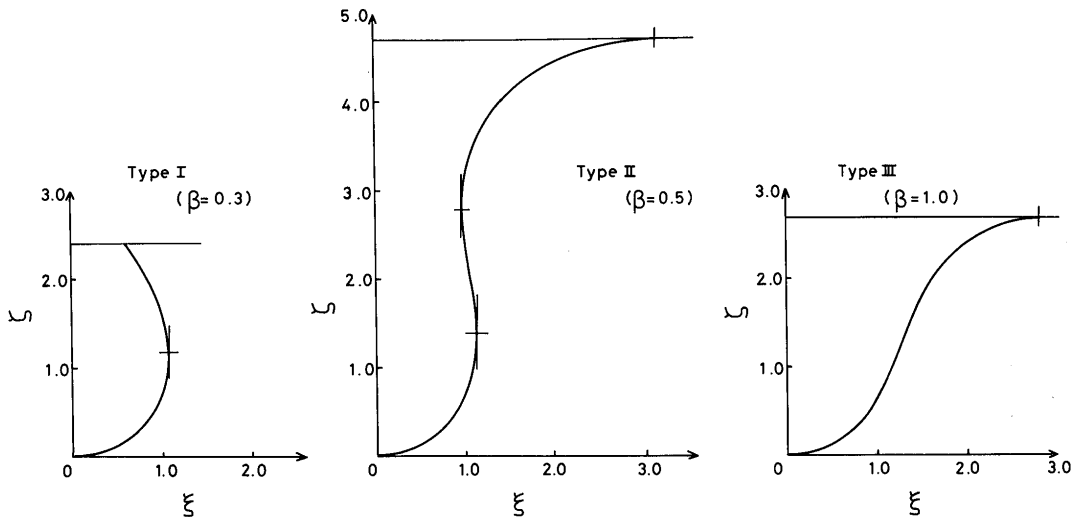

Fig. 8   Three typical profiles of pendant drops supported by cappillary pressure

trace the curve that satisfies the basic equation.

Bashforth and Adams conducted the precise calculations of eq. (18) by the above method for various cases. **Figure 8** shows some results of the calculated profile of hunging drops of liquid. There are three typical shapes of pendent drops depending on the parameter β. Each shape will be called in this paper Type I, II and III respectively. Bashforth and Adams did not comment on this characteristic differences, but if their calculated results are graphically represented, interesting features become apparent. **Figure 9** shows the characteristic sizes of a droplet when it is supported by capillary pressure. The critical values of β that changes from Type I to II and from II to III are about 0.35 and 0.62 respectively. In the β-range where Type I and II appear, the height of drop ζ_0 and its radius ξ_0 at the root changes continuously, but their tendencies are quite different in the range of Type I. If one pays an attention at the Type II region, the radius of necked part ξ_2 decreases greatly with reduction of β and on the contrary root radius ξ_0 increases remarkably. Therefore, the distinctive change at $\beta = 0.35$ seems to be related to the character of necking, but this has not been clarified yet.
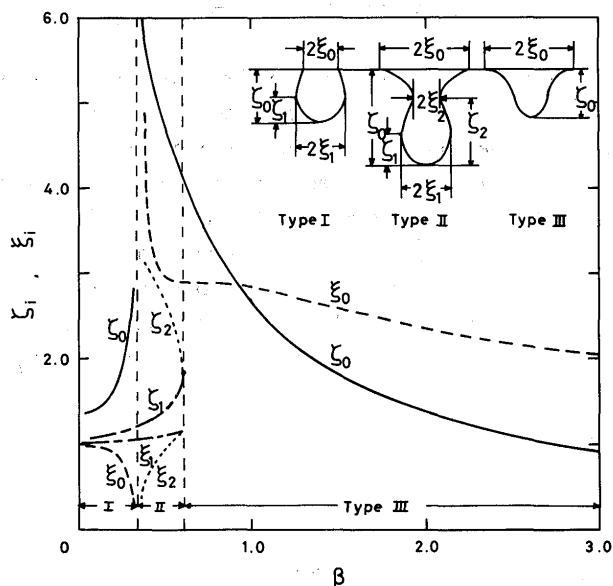

Fig. 9   Change of size parameters of pendant drops with β-index

3.2 Some investigations on metal transfer in arc welding from the view point of capillary action

In arc welding processes, the mode of liquid metal transfer from the electrode has been the subject for many researchers.[5~10] There are many forces governing the transfer in complicated manners, but their detailed interactions on a droplet formed at the electrode tip has

Table 2 IIW classification of metal transfer

Designation of Transfer Type	Welding Processes (Examples)
1 Free Flight Transfer	
1.1 Globular	
1.1.1 Drop	Low-current MIG
1.1.2 Repelled	CO_2-shielded MIG
1.2 Spray	
1.2.1 Projected	Intermediate-current MIG
1.2.2 Streaming	Medium-current MIG
1.2.3 Rotating	High-current MIG
1.3 Explosive	MMA
2. Bridging Transfer	
2.1 Short Circuiting	Short-arc MIG
2.2 Bridging without Interruption	Filler Wire Addition
3. Slag-protected Transfer	
3.1 Flux Wall Guided	SAW
3.2 Other Modes	MMA, Cored Wire, Electro-slag

MIG: Metal-Inert-Gas, MMA: Manual Metal-Arc, SAW: Submerged-Arc

not been well clarified. The mode of metal transfer is, therefore, classified by phenomenological aspect as tabulated in **Table 2**.[11] Among various transfer types, the drop transfer and bridging without interruption are usually thought to be affected dominantly by surface tension under the influence of gravity. While, other modes such as the repelled, spray (projected, streaming and rotating) and shortcircuiting transfers are regarded to be caused by electromagnetic effects.

Conventional definition of the globular and spray transfer is based on whether the maximum diameter of droplet is larger or smaller than the electrode diameter. In the MIG arc, for example, the transfer mode changes from drop transfer to projected or streaming transfer when the current is increased. As the current is small in the drop transfer mode, the electromagnetic effect may be neglected as a first order approximation. Namely, the detachment of droplet takes place when the weight exceeds the supporting force by surface tension.

Greene[9] conducted an analysis of the metal transfer in MIG welding in 1960, in which he calculated the previously mentioned profile equation (eq. (18)) in graphical method and discussed the size effect of electrode on transfer mode and its critical condition. **Figure 10 (a)** and **(b)** show the effect of electrode diameter on drop size. The maximum diameter of droplet increases with the increase in electrode radius up to about 0.85 and it keeps constant over 0.85. While, when the electrode is constant in radius, the drop size as well as the maximum volume of droplet that can be suspended decreases with the reduction of capillary constant. Greene defined the quantity

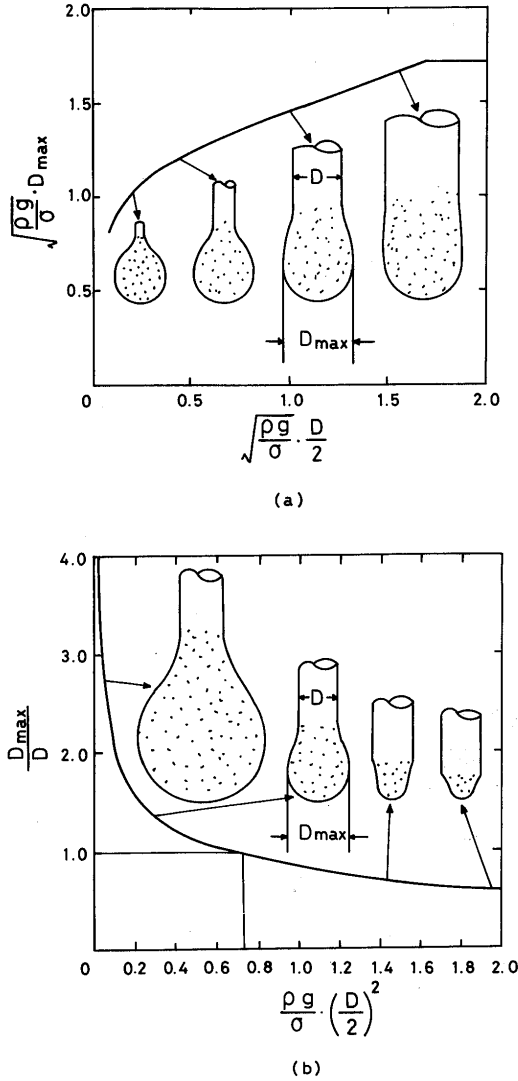$$M = \frac{\rho g}{\sigma} \left(\frac{D}{2} \right)^2 \tag{19}$$

(a)

(b)

Fig. 10 Effect of rod diameter on maximum drop diameter[9]

as Drop Size Index which is a non-dimensional area. As it is obvious in Fig. 10, the transition from drop to projected transfer takes place when $M = 0.72$ (= 0.85^2).

Here, it should be noted that Greene conducted calculations mainly in case of Type II and partly Type III mentioned in the previous section, but he put the condition that the largest drop which can be supported on the rod end must be equal to the diameter of the neck, namely, gradient of the liquid profile, $d\zeta/d\xi = \infty$ (90°) at the position of liquid-solid junction of profile curve. He also stated that if the neck diameter is less than the rod diameter, the drop could grow to a greater size before surface tension could no longer support it against gravitational forces. He did not describe any theoretical reason on this matter, but it is obvious from the Bashforth and Adams' calculation described in the previous section that this argument cannot be derived from the static pressure balance consideration. As already shown in

Fig. 8, the drop can be suspended even if the contact angle is 0. In a given profile, one can choose an arbitrary height of drop from its bottom, which means that the rod size and contact angle are not the restriction condition for the static equilibrium, as far as the profile curve of droplet intersects at the periphery of rod.

However, Ando and Hasegawa stated in their book that the hunging drop with a neck having smaller size than rod diameter might not be possible to obtain in actual case and nobody observed such shape in steady state during welding.[12] The above contradiction may be possibly resolved by considering an instability of cylindrical liquid. Lancaster[13] mentioned, in 1979, the importance of pinch instability in metal transfer.
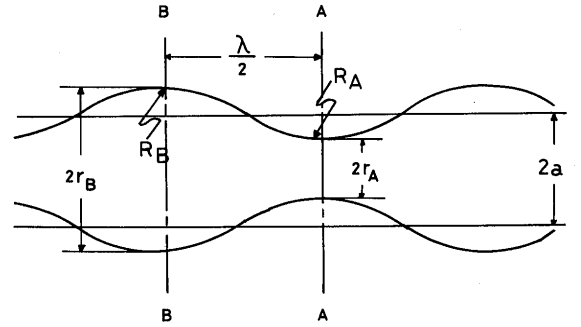

Fig. 11 Pinch instability of liquid cylinder

The simplest unstable phenomenon of self pinched liquid cylinder is so called Sausage Type Instability as shown in **Fig. 11**. If the free surface is displaced slightly from its equilibrium state, the internal pressures at the positions A and B are

$$P_A = \sigma \left(\frac{1}{r_A} - \frac{1}{R_A} \right)$$

$$P_B = \sigma \left(\frac{1}{r_B} + \frac{1}{R_B} \right)$$

If λ/a is very small, the radii of curvatures R_A and R_B are small compared to liquid radius a, and both the negative pressure at A $(-\sigma/R_a)$ and positive pressure at B (σ/R_B) act so as to recover the distorted surface to the equilibrium state. If λ/a is very large, on the other hand, R_A and R_B are large compared to a and the pressure components σ/R_A and σ/R_B can be practically neglected. Thus, the pressure at A becomes higher than that at B, since $r_A < R_B$. This pressure difference causes a liquid flow in axial direction and the diameter at A-section continues to decrease since there is no source of liquid at the position A. The reduction of radius at A, as well as the increase in radius at B, makes the pressure difference greater and the axial flow is more accelerated, and thus

the section A is finally pinched off. The pinch instability or necking of drop hunged from solid rod is analogouse to the above. However, when we consider the metal transfer, we have to take into account the Lorentz force and gravity as Lancaster has attempted.[13]

4. Summary

In succession to the previous Part 1, here were reviewed the static pressure balance of hunging liquid and its critical condition of self-support by capillary pressure. The same equation of elliptical integral described in Part 1 was used in self sustaining of root bead in flat position, and the method of Bashforth and Adams was briefed for calculating the profile of three-dimensional pendant drop, and its characteristic shapes were explained. In hunging liquids, the allowable conditions of self-sustaining by capillary action are intrinsically limited due to the gravitational force, and moreover fluidmechanical instability enhances the difficulty of supporting fluid. Two types of instabilities, Rayleigh-Taylor type instability for liquid membrane and pinch instability for pendant drop were briefly explained.

References

1) A. Matsunawa and T. Ohji: "Role of Surface Tension in Fusion Welding (Part 1)", Trans. JWRI, Osaka Univ., Vol. 11, No. 2 (1982), P. 145.

2) F. Bashforth and J.C. Adams: An Attempt to Test the Theories of Capillary Action by Comparing the Theoretical and Measured Forms of Drops of Liquid, Cambridge Univ. Press, Cambridge (1883).

3) T. Ohji: Surface Tensional Analysis on Surface Profile of Weld Bead and Sustaining of Molten Pool, Thesis for Doctorate, Osaka Univ. (1978). (in Japanese)

4) Y. Arata and K. Nishiguchi: Fundamental of Welding Processes, Sampo Pub. Co., Tokyo (1979), p. 101. (in Japanese)

5) W. Sparagen and B.A. Lengyel: "Physics of the Arc and the Transfer of Metal in Arc Welding", W.J., Vol. 22, No. 1 (1943), p. 2s.

6) O. Becken: "Metal Transfer from Welding Electrodes", IIW Doc. 212-179-69.

7) J.C. Needham, C.J. Cooksey and D.R. Milner: "Metal Transfer in Inert Gas-Shielded Arc Welding", Britsh W.J., Vol. 7, No. 2 (1960), p. 101.

8) A. Lesnewitch: "Control of Melting Rate and Metal Transfer in Gas-Shielded Metal-Arc Welding, Parts I and II", W.J., Vol. 37, No. 8 (1958), p. 343s; No. 9, p. 418s.

9) W.J. Greene: "An Analysis of Transfer in Gas-Shielded Welding Arcs", Trans. Amer. Inst. Elec. Engrs. Vo. 79, No. 49, July 1960, Pt. 2, p. 194.

10) J.C. Amson: "Lorentz Force in The Molten Tip of An Arc Electrode", British J. Appl. Phys., Vol. 16, No. 8 (1965), p. 1169.

11) IIW. Comm. XII: "Classification of Metal Transfer", IIW Doc. XII-636-76.

12) K. Ando and M. Hasegawa: Welding Arc Phenomena (Revised Ed.), Sampo Publ. Co., Tokyo (1967), p. 428. (in Japanese)

13) J.F. Lancaster: "Metal Transfer in Fusion Welding", International Conf. Proceddings on Arc Physics and Weld Pool Behaviour, The Welding Institute, Cambridge (1979), p. 135.